

# Suzaku X-Ray Spectroscopy of a Peculiar Hot Star in the Galactic Center Region

Yoshiaki HYODO,<sup>1</sup> Masahiro TSUJIMOTO,<sup>2,3\*</sup> Katsuji KOYAMA,<sup>1</sup> Shogo NISHIYAMA,<sup>4</sup>  
Tetsuya NAGATA,<sup>5</sup> Itsuki SAKON,<sup>6</sup> Hiroshi MURAKAMI,<sup>7</sup> and Hironori MATSUMOTO<sup>1</sup>

<sup>1</sup>*Department of Physics, Graduate School of Science, Kyoto University,  
Kita-shirakawa Oiwake-cho, Sakyo, Kyoto 606-8502*

<sup>2</sup>*Department of Astronomy & Astrophysics, Pennsylvania State University  
525 Davey Laboratory, University Park, PA 16802, USA*

<sup>3</sup>*Department of Physics, Rikkyo University, 3-34-1, Nishi-Ikebukuro, Toshima, Tokyo 171-8501*

<sup>4</sup>*National Astronomical Observatory of Japan, 2-21-1, Osawa, Mitaka, Tokyo 181-8588*

<sup>5</sup>*Department of Astronomy, Graduate School of Science, Kyoto University,  
Kita-shirakawa Oiwake-cho, Sakyo, Kyoto 606-8502*

<sup>6</sup>*Department of Astronomy, School of Science, the University of Tokyo, 7-3-1, Hongo, Bunkyo, Tokyo 113-0033*

<sup>7</sup>*Institute of Space and Astronautical Science, 3-1-1, Yoshinodai, Sagamihara, Kanagawa, 229-8510  
hyodo@cr.scphys.kyoto-u.ac.jp*

(Received 2007 June 12; accepted 2007 August 31)

## Abstract

We present the results of a Suzaku study of a bright point-like source in the 6.7 keV intensity map of the Galactic center region. We detected an intense FeXXV 6.7 keV line with an equivalent width of  $\sim 1$  keV as well as emission lines of highly ionized Ar and Ca from a spectrum obtained by the X-ray Imaging Spectrometer. The overall spectrum is described very well by a heavily absorbed ( $\sim 2 \times 10^{23}$  cm<sup>-2</sup>) thin thermal plasma model with a temperature of  $3.8 \pm 0.6$  keV and a luminosity of  $\sim 3 \times 10^{34}$  erg s<sup>-1</sup> (2.0–8.0 keV) at 8 kpc. The absorption, temperature, luminosity, and the 6.7 keV line intensity were confirmed with the archived XMM-Newton data. The source has a very red ( $J - K_s = 8.2$  mag) infrared spectral energy distribution (SED), which was fitted by a blackbody emission of  $\sim 1000$  K attenuated by a visual extinction of  $\sim 31$  mag. The high plasma temperature and the large X-ray luminosity are consistent with a wind-wind colliding Wolf-Rayet binary. The similarity of the SED to those of the eponymous Quintuplet cluster members suggests that the source is a WC-type source.

**Key words:** Galaxy: center — stars: Wolf-Rayet — X-rays: individual (CXOGC J174645.3–281546, 2XMMp J174645.2–281547) — X-rays: stars — X-rays: spectra

## 1. Introduction

The distribution of the 6.7 keV X-ray emission line along the Galactic plane is strongly peaked at the Galactic center (Koyama et al. 1989). The line originates from a  $K\alpha$  transition of highly ionized iron. Together with its large penetrating power delving through a  $\approx 10^{24}$  H cm $^{-2}$  extinction, the emission is an indispensable tool to trace the high-energy activity and to reveal the X-ray source demographics in a heavily attenuated environment, such as the Galactic center region, where the enormous density of gas and dust, the strong magnetic fields, and the existence of a super massive black hole influence every aspect of the transmigration of energy and matter (Morris & Serabyn 1996).

Both the extended emission and the ensemble of numerous discrete sources contribute to the 6.7 keV emission. The nature of the extended emission was identified as a hot plasma having a temperature of  $\sim 6.5$  keV, distributed across  $\sim 250$  pc (Koyama et al. 1989, 2007c). For discrete sources, several different X-ray populations with thermal emission play dominant roles.

Cataclysmic variables (CV), binaries of a white dwarf and predominantly a late-type dwarf star, are major contributors to the 6.7 keV line, considering its large population and thermal plasma with emission lines (Ezuka & Ishida 1999; Munro et al. 2003, 2004b). Low-mass young stellar objects (YSO) or pre-main-sequence late-type sources are other types of candidates. They have elevated X-ray activity compared to their main-sequence phases, and show a hard thermal X-ray emission with the 6.7 keV line both during the occasional flare and quiescent phases (Koyama et al. 1996a; Tsuboi et al. 1998; Imanishi et al. 2001; Ozawa et al. 2005). They are expected to be numerous in the Galactic center region, where  $\sim 10\%$  of the star formation of the entire Galaxy takes place (Figer et al. 2004).

In addition to these late-type populations, early-type sources are also expected to contribute to the 6.7 keV emission. Main-sequence field O-type stars do not show hard X-ray emission with their plasma temperatures below  $\sim 1$  keV (Berghoefer et al. 1997), but recent observations reveal that some main-sequence O-type stars in OB associations show hard thermal X-ray emissions of  $\gtrsim 2$  keV (Tsujiimoto et al. 2007b and references therein). Intense 6.7 keV line emissions are confirmed from such sources (Albacete Colombo et al. 2003, 2007; Broos et al. 2007; Hyodo et al. 2008). Early-type sources are extremely rare compared to late-type sources in number, but their overwhelmingly large luminosity can be comparable to the integrated luminosity of numerous late-type sources. In the Orion Nebula Cluster, for instance, an O6V star ( $\theta^1$  Ori C) alone accounts for  $\sim 34\%$  of the total hard-band X-ray emission integrated over the entire Chandra field of view containing  $> 1000$  YSOs (Feigelson et al. 2005).

Early-type stars become even brighter in X-rays when they evolve off the main-sequence track. Wolf-Rayet (WR) stars and Luminous Blue Variables (LBVs) comprise the bright-

---

\* Chandra Fellow

est X-ray population of thermal point-like sources with a typical hard-band luminosity of  $\sim 10^{34}$  erg s $^{-1}$  and a plasma temperature of  $\gtrsim 2$  keV (Koyama et al. 1994; Tsuboi et al. 1997; Portegies Zwart et al. 2002b; Wang et al. 2006). In fact, the brightest stellar X-ray source not powered by accretion reported to date in our Galaxy is a WR star of a spectral type of WN7–8 in the Arches cluster (A1S in Yusef-Zadeh et al. 2002; Law & Yusef-Zadeh 2004; Wang et al. 2006; Tsujimoto et al. 2007a). The source has the 0.2–10.0 keV luminosity exceeding  $\sim 10^{35}$  erg s $^{-1}$  with a conspicuous 6.7 keV emission. Moreover, the X-ray spectra of these stars commonly show strong metallic emission lines against continuum including the 6.7 keV line, which is a consequence of extreme hydrogen depletion caused by the mass loss and hydrogen burning (van der Hucht et al. 1986).

Although early-type stars known in the Galactic center region are concentrated to the three massive young star clusters — the Arches (Nagata et al. 1995; Cotera et al. 1996; Serabyn et al. 1998; Figer et al. 1999b), the Quintuplet (Kobayashi et al. 1983; Okuda et al. 1990; Nagata et al. 1990; Figer et al. 1999a), and the Central cluster (Becklin & Neugebauer 1968; Krabbe et al. 1995; Ghez et al. 2005) —, it is quite natural to expect that a much larger number of early-type stars remain unidentified. Portegies Zwart et al. (2001) claimed that the number of young massive star clusters may exceed 50 in the Galactic center region. The inconsistency with the observed value indicates that these clusters are too obscured to be visible in the optical and infrared bands, or that the cluster members are dissipated before the earliest member reaches its end, or that that number is a gross overestimate. Kim et al. (1999) showed that the strong tidal disruption in the Galactic center region makes massive star clusters become unbound on a very short time scale comparable to the lifetime of an O star. Isolated early-type stars may be distributed throughout the region, unlike the other parts of the Galaxy where they are found in associations.

Some early attempts have been made to discover unidentified early-type stars in the Galactic center region with the combination of X-ray and infrared (IR) observations. Munro et al. (2006a) made trailblazing observations of radio, IR, and X-ray to reveal the population of young massive stars in the Galactic center region. They detected strong Br $\gamma$  and HeI lines from two sources, and classified them as either Of or candidate LBV stars. Mauerhan et al. (2007) also conducted *K*-band spectroscopy of six bright hard X-ray sources with very red IR colors. Two of them, with IR colors of  $J-K = 4-5$  mag, show broad hydrogen and helium emission lines characteristic of evolved O-type stars. They are classified as a Wolf-Rayet star of a spectral type of WN6 and an O-type Ia supergiant. Likewise, Mikles et al. (2006) performed infrared spectroscopy of CXO J174536.1–285638, which is one of new Chandra sources discovered by Munro et al. (2003). They detected P Cygni profiles of HeII lines of a 170 km s $^{-1}$  wind. The spectral features in the X-ray and IR bands are most consistent with the colliding wind binary system  $\eta$  Car. This source is of particular interest in terms of a strong FeXXV emission line, which is also prominent in our source, presented below. We see a high prospect of these methods

**Table 1.** Observation log.

Start Date	Observatory	ObsID	R. A. (J2000.0)	Decl.	$t_{\text{exp}}^*$ (ks)	$\theta^\dagger$ (')
2000-09-23	XMM-Newton	0112970201	17 <sup>h</sup> 47 <sup>m</sup> 21 <sup>s</sup>	-28°09'02''	11	11.7
2000-10-27	Chandra	1036	17 <sup>h</sup> 47 <sup>m</sup> 22 <sup>s</sup>	-28°11'36''	35	10.5
2001-07-16	Chandra	2271	17 <sup>h</sup> 47 <sup>m</sup> 28 <sup>s</sup>	-28°16'29''	10	9.5
2001-07-16	Chandra	2274	17 <sup>h</sup> 46 <sup>m</sup> 42 <sup>s</sup>	-28°10'23''	10	5.7
2001-07-16	Chandra	2285	17 <sup>h</sup> 46 <sup>m</sup> 18 <sup>s</sup>	-28°20'23''	10	7.9
2003-03-12	XMM-Newton	0144220101	17 <sup>h</sup> 47 <sup>m</sup> 23 <sup>s</sup>	-28°09'15''	34	10.4
2006-09-21	Suzaku	501040010	17 <sup>h</sup> 46 <sup>m</sup> 46 <sup>s</sup>	-28°22'51''	70	7.4
2006-09-24	Suzaku	501040020	17 <sup>h</sup> 46 <sup>m</sup> 46 <sup>s</sup>	-28°22'51''	50	7.4

\* Exposure time after removing periods with high background level. The exposure times for the XMM-Newton observations refer to those obtained with the EPIC-pn camera.

† Angular distance of the source from the optical axis.

to find similar sources en masse.

Near-IR spectroscopy may confront a challenge for even redder sources. In addition to a  $\sim 30$  mag visual extinction ubiquitous toward the Galactic center region (Catchpole et al. 1990; Schultheis et al. 1999), evolved early-type stars are behind an additional local extinction by their own mass loss. Photospheric emission is reprocessed into longer wavelength radiation in the optically thick circumstellar matter. The IR spectra turn out to be featureless by strong veiling (Figer et al. 1999a; Crowther et al. 2006). For such sources, the spectroscopy of the hard X-ray emission directly from the vicinity of the star is the only practical tool. These stars contribute to the 6.7 keV line emission, and the diagnosis of the line emission helps to identify their nature.

Here, we present the results of a Suzaku (Mitsuda et al. 2007) study of an X-ray point-like source located at a  $\sim 100$  pc projected distance from the Galactic center. The source is exceptionally bright in the 6.7 keV map of the region, and is redder ( $J-K > 8$  mag) than those studied in previous studies. Aided by the large effective area of Suzaku's telescope to produce spectra having high photon statistics, we conducted a detailed hard-band spectroscopy of this source to identify its nature.

## 2. Observation and Data Reduction

As a part of the Suzaku mapping campaign of the Galactic center region, a field containing the Sgr B2 molecular cloud was observed twice on 2006 September 21–23 and 24–25 with an aim point at (RA, Dec) = (17<sup>h</sup>46<sup>m</sup>46<sup>s</sup>, -28°22'51''). The observation log is given in table 1. Suzaku observations produce two simultaneous data sets using the X-ray Imaging Spectrometer (XIS: Koyama et al. 2007a) and the Hard X-ray Detector (HXD: Kokubun et al.

2007; Takahashi et al. 2007). We concentrate on the former in this paper.

The XIS is equipped with four X-ray charge coupled devices (CCDs) at the foci of four X-Ray Telescopes (XRT: Serlemitsos et al. 2007). Each CCD chip has a format of  $1024 \times 1024$  pixels. The four XRTs are aligned to observe the same field of  $\sim 18' \times 18'$  with a half-power diameter (HPD) of  $1.9\text{--}2.3$  and a pointing accuracy of up to  $\sim 50''$ . Three of the four chips (XIS0, 2, and 3) are front-illuminated (FI) CCDs superior in the hard band response covering the 0.4–12 keV energy range. The remaining one is a back-illuminated (BI) CCD superior in the soft band covering 0.2–12 keV. The total effective area is  $\sim 550 \text{ cm}^2$  at 8 keV.

The energy resolution, initially of  $\sim 130 \text{ eV}$  at 6 keV in the full width at half maximum, is subject to degradation due to cosmic-ray radiation in the orbit. The XIS employs two techniques to calibrate and rejuvenate its spectral capability. One is standard radioactive sources. Two  $^{55}\text{Fe}$  sources are installed to illuminate two corners of each CCD to calibrate the absolute energy gain. The other is the spaced-row charge injection (SCI). Electrons are injected at one of every 54 rows, and are transferred through columns to sacrificially fill in traps caused by radiation. This reduces the number of trapped charges by X-ray events throughout the transfer, thus improving the energy resolution (Bautz et al. 2004; Koyama et al. 2007a).

The observations were conducted using the normal clocking mode with a frame time of 8 s. The SCI technique was used. Data process version 1.2<sup>1</sup> was retrieved and events were removed during the South Atlantic Anomaly passages and at earth elevation angles below 3 degrees. After the filtering, the combined net integration time is  $\sim 120 \text{ ks}$ .

Because the calibration database for SCI observations is not yet released as of this writing, we used data obtained during the ground calibration with a charge-transfer efficiency of 1. Using the Mn  $K\alpha$  line from the calibration sources ( $^{55}\text{Fe}$ ), we measured the systematic gain offset as the deviation from the theoretical value at 5.8951 keV (Bearden 1967; Krause & Oliver 1979). The offsets were found to be within  $\sim 10 \text{ eV}$  for the FI and  $\sim 30 \text{ eV}$  for the BI chips.

### 3. Analysis

#### 3.1. Images

Figure 1 shows XIS images of the study field in the (a) 0.7–2.0 and (b) 2.0–7.0 keV bands. The overlaid contours in (a) are the narrow-band intensity in 6.75–6.77 keV. All four XIS images at the two observations are combined. Several distinctive features can be found in the hard band. Two extended sources are Sgr B2 (Koyama et al. 1996b, Murakami et al. 2000, 2001; Koyama et al. 2007b) and G0.61–0.01 (Koyama et al. 2007b). The brightest source, which is the main topic of this paper, is found close to the northern edge of the hard-band image. The source is point-like and an exceptionally intense 6.7 keV emitter in the image, and

---

<sup>1</sup> See <http://www.astro.isas.jaxa.jp/suzaku/process/history/v1225.html>.

**Table 2.** Best-fit spectral parameters.\*

Parameter	Unit	Suzaku	XMM-Newton
$N_{\text{H}}$	$(10^{23} \text{ cm}^{-2})$	$2.4^{+0.3}_{-0.2}$	$2.3^{+0.4}_{-0.3}$
$k_{\text{B}}T$	(keV)	$3.8^{+0.5}_{-0.6}$	$3.8^{+0.7}_{-0.7}$
$Z_{\text{Ar}}$	(solar)	$8.7^{+6.3}_{-4.9}$	$2.9^{+7.1}_{-2.9}$
$Z_{\text{Ca}}$	(solar)	$3.2^{+2.3}_{-2.0}$	$0.9^{+2.8}_{-0.9}$
$Z_{\text{Fe}}$	(solar)	$0.8^{+0.1}_{-0.1}$	$0.9^{+0.2}_{-0.2}$
$F_{\text{X}}^{\dagger}$	$(10^{-12} \text{ erg s}^{-1} \text{ cm}^{-2})$	$1.00^{+0.03}_{-0.03}$	$1.05^{+0.07}_{-0.07}$
$L_{\text{X}}^{\ddagger}$	$(10^{34} \text{ erg s}^{-1})$	2.8	2.9
$\chi^2/\text{d.o.f.}$		89.4/106	69.9/74

\* The uncertainty indicates the 90% confidence ranges of the fit.

$\dagger$  Energy flux in the 2.0–8.0 keV band.

$\ddagger$  Absorption-corrected luminosity in the 2.0–8.0 keV band. A distance of 8 kpc is assumed.

also in the vicinity found in the Suzaku wide-field map.

### 3.2. Spectra

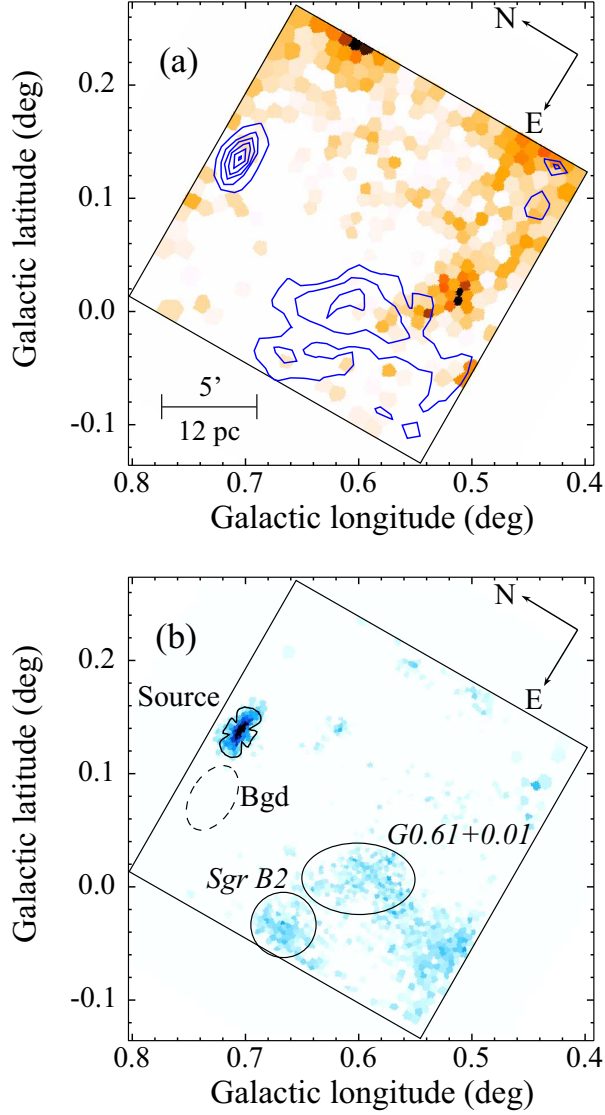
We extracted the source and background events from the polygonal and elliptical regions, respectively (figure 1b). The source was superimposed upon the intense diffuse emission ubiquitous in the Galactic center region (Koyama et al. 1996b). In order to maximize the signal-to-noise ratio against the underlying emission, we simulated point spread functions at the source position with different enclosed energy fractions using a ray-tracing simulator (**xissim**: Ishisaki et al. 2007). Consequently, a 60% encircled energy polygon was chosen to accumulate source photons. The background region was selected from an ellipse adjacent to and at a similar off-axis angle with the source region.

Figure 2 shows the background-subtracted spectrum. Here, we generated the telescope response files using a ray-tracing simulator (**xissimarfgen**: Ishisaki et al. 2007). We used the detector response files as of 2005 August, which best describe the spectral profiles of the calibration sources.

The spectrum is characterized by several emission lines as well as a hard continuum extending to  $\sim 10$  keV with a strong soft-band cut-off. The lines are identified as  $K\alpha$  emission from highly ionized (He-like and H-like) ions of Ar, Ca, and Fe. The spectrum was first fitted by a bremsstrahlung model with Gaussian lines attenuated by interstellar extinction (Morrison & McCammon 1983). The strongest line is He-like Fe  $K\alpha$  at  $6.66 \pm 0.01$  keV with an energy flux of  $(2.5 \pm 0.3) \times 10^{-13} \text{ erg s}^{-1} \text{ cm}^{-2}$ , which corresponds to an equivalent width (EW) of  $950 \pm 100$  eV.

In contrast, the line feature at 6.4 keV, if present, is very weak. We added a narrow Gaussian line at the energy and derived a 90% upper limit of  $1.5 \times 10^{-14} \text{ erg s}^{-1} \text{ cm}^{-2}$ , which





**Fig. 1.** XIS images in the (a) 0.7–2.0 and (b) 2.0–7.0 keV bands. The narrow-band intensity of 6.57–6.77 keV is shown in (a) by contours. The source and background regions are respectively shown by a polygon and a dashed ellipse in (b). Both images were processed (1) to mask calibration sources, (2) to subtract non-X-ray background signals constructed from night earth observations (Tawa et al. 2008), (3) to correct for the vignetting and the non-uniformity caused by the contamination material on the optical blocking filter, (4) to resample adaptively to achieve a signal-to-noise ratio of  $> 8$  at each bin using the weighted Voronoi tessellation algorithm (Diehl et al. 2006, Cappellari et al. 2003), and (5) to register the coordinate using the Chandra counterpart of the point-like source.

corresponds to an EW of 50 eV. The temperature derived from the continuum and those from the intensity ratios of He-like and H-like  $K\alpha$  lines are consistent with  $\sim 4$  keV, indicating that the emission is thermal plasma in collisional equilibrium.

We then fitted the spectrum with an optically-thin thermal plasma model (APEC: Smith et al. 2001) with interstellar extinction (Morrison & McCammon 1983). The abun-

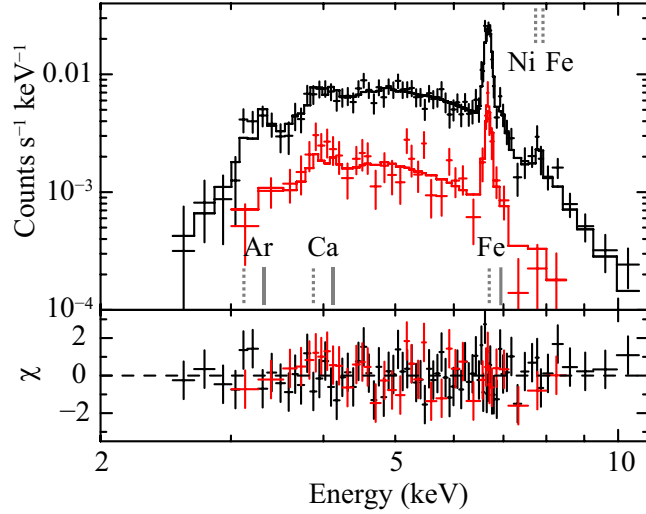


**Fig. 2.** Background-subtracted XIS spectra. BI spectrum is shown in red, while the merged FI spectrum is in black. The upper panel shows the data with crosses and the best-fit APEC models with solid lines, while the lower panel shows the residuals to the best-fit. Conspicuous emission lines of He-like ions (gray dash lines) and H-like ions (gray solid lines) are labeled.

dances of Ar, Ca, and Fe relative to solar were free parameters, while the other elements were fixed to 1 solar abundance (Anders & Grevesse 1989). A single-temperature model yielded an acceptable fit with 3.8 keV in plasma temperature ( $k_B T$ ),  $1.0 \times 10^{-12}$  erg s $^{-1}$  cm $^{-2}$  in X-ray flux ( $F_X$ ) in the 2.0–8.0 keV band and  $2.4 \times 10^{23}$  cm $^{-2}$  in hydrogen column extinction ( $N_H$ ). The best-fit model and values are shown in figure 2 and table 2, respectively. No systematic deviation was found in the single temperature fit, requiring no extra components.

To examine how the results are influenced by our choice of the background region, we repeated the same procedures with several different regions. All the best-fit parameters are consistent with each other, except for the X-ray flux, which suffers  $\lesssim 10\%$  systematic uncertainty.

### 3.3. *Chandra and XMM-Newton Counterparts*

We retrieved the archived Chandra (Weisskopf et al. 2002) and XMM-Newton (Jansen et al. 2001) data to study the long-term behaviors of the source, and to locate its position more precisely using telescopes of smaller HPDs than that of Suzaku. Four Chandra observations using the Advanced CCD Imaging Spectrometer (ACIS: Garmire et al. 2003) and two XMM-Newton observations using the European Photon Imaging Camera (EPIC: Turner et al. 2001; Strüder et al. 2001), which is comprised of two MOS and a PN, were found to cover the Suzaku source (table 1).

Within the Suzaku positional uncertainty of 50'', we found only one Chandra source (CXOGC J174645.3–281546) in Munro et al. (2006b) and one XMM-Newton source (2XMMp J174645.2–281547) in the Second XMM-Newton Serendipitous Source Pre-release



Catalogue, XMM-Newton Survey Science Centre (2006). Also, hereafter we refer the Suzaku source as CXOGC J174645.3–281546.

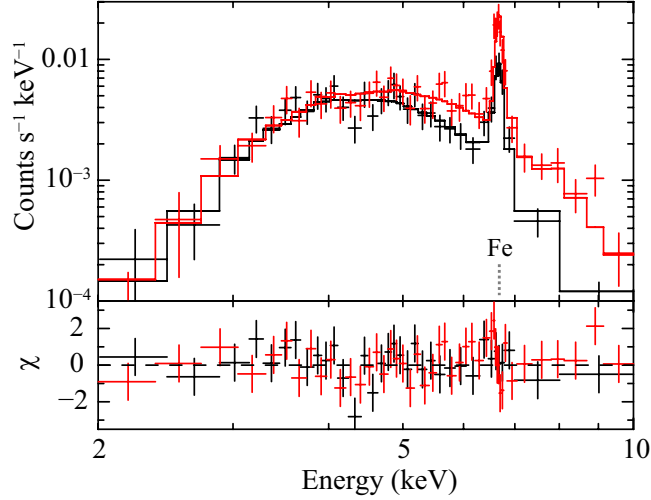


**Fig. 3.** Background-subtracted EPIC spectra. The pn spectrum is shown in red, while the merged MOS spectrum is in black. The symbols follow figure 2.

Since no spectroscopic and temporal behaviors are presented for both of the Chandra and XMM-Newton sources in the literature, we analyzed the data and present the results here. One of the two XMM-Newton observations showed a net exposure of  $\sim 34$  ks after removing data during high background. Spectra with high statistics were obtained from MOS and PN, for which we conducted spectral fits in a similar manner as with the Suzaku spectrum. The best-fit model and parameters are shown in figure 3 and table 2, respectively. Although the emission lines are less conspicuous in the XMM-Newton data, the Suzaku and XMM-Newton results are consistent with each other.

For the remaining one XMM-Newton and four Chandra observations, the photon statistics were too poor for a detailed spectral analysis, due to short exposures, chip gaps, and large off-axis angles of the source position. We therefore applied the best-fit Suzaku model to derive their flux.

Figure 4 shows a long-term flux variation, which spans  $\sim 6$  years at seven different epochs. Although no flux variation within each observation is found, a long-term variation having a factor  $\sim 2$  is clearly found.

### 3.4. Longer Wavelength Data

We retrieved other databases to characterize the multi-wavelength features of CXOGC J174645.3–281546. Because of the extreme extinction, the source is inaccessible in the optical bands. In the near-infrared (NIR) bands, we examined the Two Micron All-Sky Survey (2MASS: Cutri et al. 2003; Skrutskie et al. 2006) and the NIR Galactic center survey

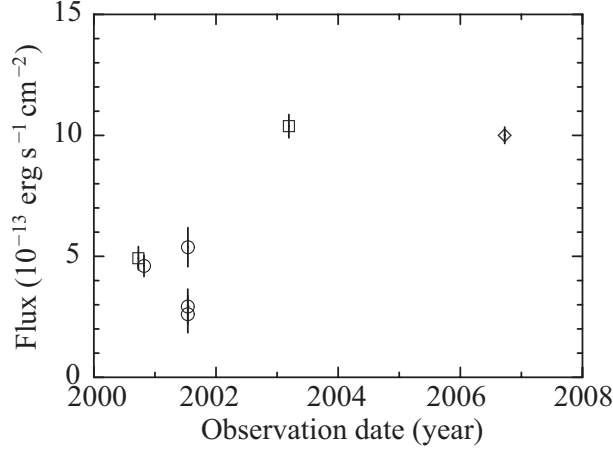


**Fig. 4.** Long-term trend of X-ray flux in the 2.0–8.0 keV using XMM-Newton (squares), Chandra (circles), and Suzaku (a diamond). Error bars on the data points are plotted at the 90% confidence level.

(Nishiyama et al. 2006) using Simultaneous Infrared Imager for Unbiased Survey (SIRIUS: Nagashima et al. 1999; Nagayama et al. 2003) on the Infrared Survey Facility (IRSF) telescope. In the mid-infrared (MIR) bands, we used the Midcourse Space Experiment (MSX: Egan et al. 2003) and the Galactic Legacy Infrared Mid-Plane Survey Extraordinaire program (GLIMPSE: Benjamin et al. 2003) using the Spitzer Space Telescope (Werner et al. 2004).

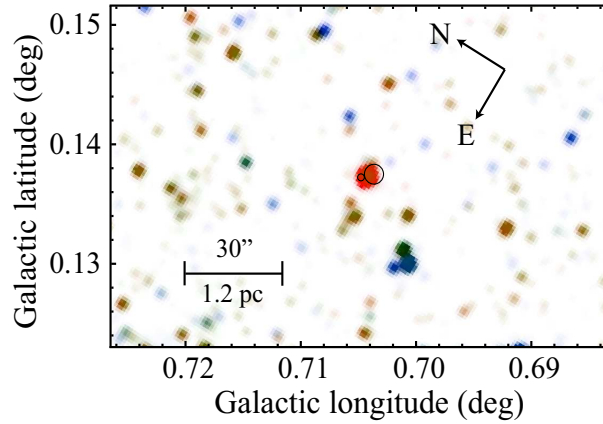


**Fig. 5.** NIR pseudo-color image using 2MASS  $J$ - (blue),  $H$ - (green), and  $K_s$ - (red) band images. The source positions with the uncertainty of Chandra and MSX are shown with a small and large circle, respectively.

Figure 5 shows an NIR pseudo-color image, in which an isolated point-like source (2MASS J17464524–2815476 and MSX C6 G000.7036+00.1375) is found in the 2MASS and MSX images within the positional uncertainty range of the Chandra source. The source is very bright and red with 2MASS magnitudes of  $(J, H, K_s) = (> 15.4, 10.0, > 7.2)$  mag. The  $J$ - and  $K_s$ -band magnitudes are upper limits due to nearby source contamination. In the SIRIUS data, while the  $K_s$ -band is unavailable due to saturation, the magnitudes of  $(J, H) = (15.53, 10.05)$

were derived with photometric errors of  $\sim 0.01$  mag.

In the MIR bands, the source is in the linearity range in the MSX photometry, but is too bright in Spitzer images, from which no meaningful photometry was obtained. Figure 6 shows the spectral energy distribution (SED) in the 1.2–30  $\mu\text{m}$  band. We fitted the data with a single-temperature blackbody and an assumed extinction proportional to the inverse square of the wavelength. We found a best-fit blackbody temperature ( $T_{\text{BB}}$ ) of  $980 \pm 20$  K, with a visual extinction ( $A_V$ ) of  $31 \pm 1$  mag, and a bolometric luminosity ( $L_{\text{bol}}$ ) of  $(8.3 \pm 0.5) \times 10^4 L_{\odot} (d/8.0 \text{ [kpc]})^2$ .

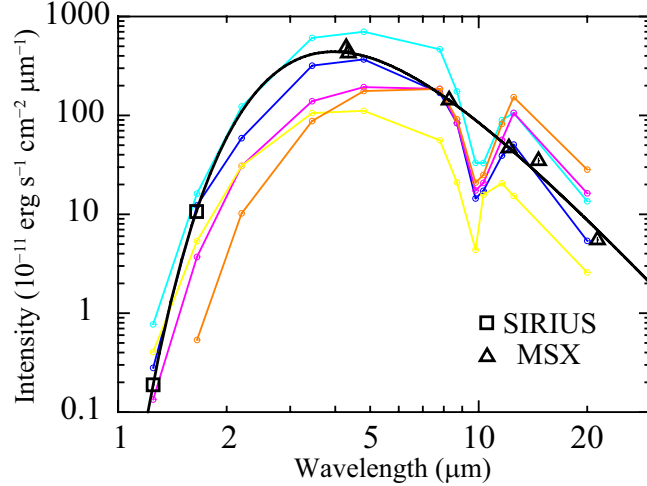


**Fig. 6.** SED constructed from SIRIUS (open squares) and MSX (open triangles) photometry. The solid curve shows the best-fit blackbody model with  $T_{\text{BB}} = 980$  K,  $A_V = 31$  mag and  $L_{\text{bol}} = 8.3 \times 10^4 L_{\odot}$ . SEDs of the eponymous Quintuplet cluster members (Okuda et al. 1990; Figer et al. 1999a) are also shown with colors for comparison.

## 4. Discussion

### 4.1. Location of Extinction Matter

Adopting  $N_{\text{H}}/A_V = 1.79 \times 10^{21} \text{ cm}^{-2} \text{ mag}^{-1}$  (Predehl & Schmitt 1995),  $A_V = 31$  mag is converted to  $N_{\text{H}} \sim 5.6 \times 10^{22} \text{ cm}^{-2}$ . This is far smaller than that determined with the X-ray of  $N_{\text{H}} \sim 2.4 \times 10^{23} \text{ cm}^{-2}$ . Since the visual extinction of 31 mag is the typical value toward the Galactic center (Catchpole et al. 1990), the excess X-ray absorption is probably due to local obscuring matter that radiates the detected IR emission. If such an obscuring matter with solar abundance spherically surrounds the X-ray source, the 6.4 keV line with an EW of  $\sim 200$  eV should be detected (Inoue 1985). The lack of 6.4 keV line ( $\text{EW} < 50$  eV) requires either that the iron abundance is  $\lesssim 0.25$  solar or that the local matter is concentrated in front of the source along the line of sight.

## 4.2. Nature of the Source

### 4.2.1. WR Binary Origin

The SED of CXOGC J174645.3–281546 in the IR bands is very similar to those of the eponymous Quintuplet cluster members (figure 6). The five stars have cool ( $T \sim 1000$  K) spectra and are bright ( $\sim 7$  mag in the  $K$ -band). The deep absorption at  $\sim 10 \mu\text{m}$  is due to interstellar silicate. The lack of either emission lines or intrinsic absorption features (Okuda et al. 1989; Figer et al. 1999a) allows no spectral classification, though their luminosity of  $\sim 10^5 L_\odot$  corresponds to those of supergiant stars. These intriguing stars were recently spatially resolved (Tuthill et al. 2006). Two (GCS 3–2 and GCS 4 of Nagata et al. 1990, or Q2 and Q3 of Moneti et al. 2001) out of five showed beautiful pinwheel nebulae of dust plume, which are seen in a few WC (carbon rich Wolf-Rayet) stars (Tuthill et al. 1999; Monnier et al. 1999). Circumstellar dust emission with temperatures of 700–1700 K is a common character of WC stars (Williams et al. 1987).

Interestingly, the two sources that exhibit the pinwheel morphology are the brightest hard X-ray sources (Law & Yusef-Zadeh 2004; Wang et al. 2006) among the Quintuplet members. Since both the pinwheel dust plumes and the hard X-ray emissions indicate fast wind-wind collision (Tuthill et al. 1999; Monnier et al. 1999; Oskinova et al. 2003), this coincidence is not probably accidental. The summed spectrum of three X-ray emitting sources (GCS 3-2, GCS 4, and source D of Nagata et al. 1990) in the Quintuplet cluster is very hard ( $kT \sim 9$  keV) and shows a hint of iron K emission line, but the luminosity is smaller by  $\sim 2$  orders of magnitude ( $7.6 \times 10^{32}$  erg s $^{-1}$  in the 0.3–8.0 keV band; Wang et al. 2006) than CXOGC J174645.3–281546. In the colliding wind binary scenario, the X-ray luminosity scales as  $L_X \propto D^{-1}$  (Stevens et al. 1992), where  $D$  is the binary orbital separation. The large X-ray luminosity of CXOGC J174645.3–281546 indicates the close separation, and the moderate flux variation having a factor of  $\sim 2$  can be interpreted as the variation of the separation due to the orbital motion.

Some of evolved massive star+OB star systems have very large X-ray luminosity up to  $\sim 10^{35}$  erg s $^{-1}$  in the 0.5–10.0 keV band with thermal spectra with a temperature of  $\gtrsim 2$  keV and an iron abundance of 1–2 ( $\eta$  Carinae: Tsuboi et al. 1997, Hamaguchi et al. 2007; WR 140: Koyama et al. 1994, Pollock et al. 2005, A1 S, A1 N, and A2 in the Arches cluster; Wang et al. 2006). The X-ray spectral property of CXOGC J174645.3–281546 coincides with those of these massive star binaries, though near- and mid-IR spectroscopy and high spatial resolution observation are essential for further constraint. Taking the discussion in §4.1. into account, all of the observational results are consistent with the idea that CXOGC J174645.3–281546 is a WC star+massive star binary near the Galactic center, which has local obscuring matter (figure 7).

Because the initial mass of a WR star exceeds  $\sim 40 M_\odot$  and the age is less than  $\sim 6$  Myr (Maeder & Meynet 1987), we naturally expect that WR stars are found in large young star clusters, assuming a usual initial mass function. Our source, however, seems to be isolated

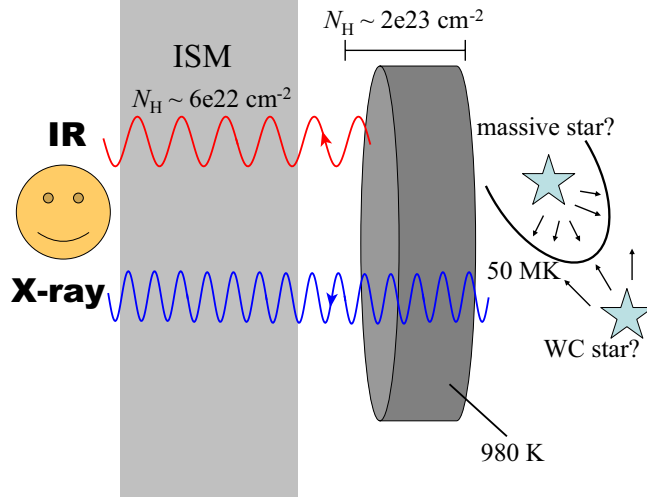


**Fig. 7.** Cartoon of the source system. Winds from the primary WC star and the companion massive star collide to produce X-rays. The obscuring material of  $N_{\text{H}} \sim 2 \times 10^{23} \text{ cm}^{-2}$  around the binary system is heated to  $T \sim 980 \text{ K}$  by photospheric emission to emit IR. Whereas the IR emission suffers only interstellar medium (ISM) extinction, the X-ray emission is subject to additional intrinsic absorption.

(figure 5). Munro et al. (2006a) and Mauerhan et al. (2007) also recently discovered such isolated massive stars in the Galactic center region. One possibility is that these stars were formed initially in a cluster, and the cluster dissipated due to the strong tidal force of the Galactic center (Portegies Zwart et al. 2002a). Future IR and X-ray observations with a higher spatial resolution and sensitivity may reveal that either this source is really a cluster member, or truly an isolated star.

#### 4.2.2. Other Possible Origins

The most popular class of hard X-ray sources that exhibits iron K-shell emission lines is CV. The X-ray luminosity of CXOGC J174645.3–281546 of  $3 \times 10^{34} \text{ erg s}^{-1}$  is at the brightest end of CVs. The bolometric luminosity of  $\sim 10^5 L_{\odot} (d/8.0 \text{ [kpc]})^2$  is, however, far larger than CVs, because most of the optical companions of CVs are late-type main-sequence stars. The spectra of CVs are characterized by hard continuum, with three iron K-shell emission lines at 6.4 keV, 6.7 keV, and 6.97 keV. The equivalent widths of both the 6.4 keV and 6.7 keV lines are, however, around 100–200 eV, although in some cases that of the 6.7 keV line shows an exceptionally high value possibly due to resonance scattering (Terada et al. 2001). The 6.97 keV/6.7 keV flux ratio of CVs is larger than 0.1, indicating that the ionization temperature is higher than  $\sim 4 \text{ keV}$  (Ezuka & Ishida 1999; Hellier & Mukai 2004; Rana et al. 2006). CXOGC J174645.3–281546 has a significantly larger equivalent width of the 6.7 keV line ( $\sim 1 \text{ keV}$ ) and lower flux ratio of the 6.97 keV/6.7 keV lines than those of CVs. The upper limit of 50 eV for the 6.4 keV line, on the other hand, can not give any constraint on the possibility of a CV. Altogether, CXOGC J174645.3–281546 is very unlikely to be a CV.

The X-ray spectra of YSOs are characterized by a thin thermal plasma with a tempera-

ture of 1–5 keV and a metal abundance of around 0.3 solar in the quiescent phase (Feigelson et al. 2002; Imanishi et al. 2003; Ozawa et al. 2005). The CXOGC J174645.3–281546 iron abundance of  $0.8 \pm 0.1$  solar is higher than the typical YSO value of 0.3 solar, but is not exceptional. Although the ratio of the X-ray and bolometric luminosity ( $L_X/L_{\text{bol}}$ ) of  $10^{-5}$  is in the range of low-mass YSOs (Imanishi et al. 2001; Feigelson et al. 2002), the absolute luminosities are too high for a YSO if CXOGC J174645.3–281546 is located at 8 kpc. The possibility still remains that CXOGC J174645.3–281546 is a foreground YSO in a dense molecular cloud.

#### 4.3. Contribution to the Galactic Center 6.7 keV Line

The 6.7 keV line flux from CXOGC J174645.3–281546 is  $2.5 \times 10^{-13} \text{ erg s}^{-1} \text{ cm}^{-2}$ . The total flux of iron K-lines in the Galactic center region is  $\sim 1.3 \times 10^{-10} \text{ erg s}^{-1} \text{ cm}^{-2}$  (Yamauchi et al. 1990). Since this value includes the 6.4 keV and 6.97 keV lines, it overestimates the 6.7 keV flux by a factor of 2–3. The detected point sources account for  $\sim 10\%$  of the total flux of the 6.7 keV line (Wang et al. 2002; Munro et al. 2004a). Therefore, the 6.7 keV line of CXOGC J174645.3–281546 alone accounts for  $\sim 4\%$  of that of the detected point sources and  $\sim 0.4\%$  of that of the total diffuse flux. Such X-ray sources would comprise a substantial fraction of 6.7 keV line-emitting point sources in the Galactic center.

## 5. Summary

1. We detected a strong 6.7 keV line with an equivalent width of  $\sim 1$  keV from CXOGC J174645.3–281546. The overall spectrum was very well fitted by a heavily absorbed ( $N_{\text{H}} \sim 2.4 \times 10^{23} \text{ cm}^{-2}$ ) 3.8 keV thermal plasma with an iron abundance of  $\sim 0.8$  solar and a luminosity of  $\sim 3 \times 10^{34} \text{ erg s}^{-1}$  in the 2.0–8.0 keV band, assuming a distance of 8 kpc.
2. We also analyzed the archived data of Chandra and XMM-Newton, and found that the X-ray flux spanning  $\sim 6$  years shows year-scale time variability having a factor of  $\sim 2$ .
3. The probable counterpart in the IR bands is very bright ( $L_{\text{bol}} \sim 10^{4.9} L_{\odot}$  at 8 kpc), and has a cool ( $T_{\text{BB}} \sim 1000 \text{ K}$ ) SED, which is similar to those of the eponymous members of the Quintuplet cluster.
4. The X-ray spectral and temporal properties and the IR SED are fully consistent with a WC star+massive star binary system.

Y. H. and M. T. acknowledge financial support from the Japan Society for the Promotion of Science. The work is financially supported by the grants-in-aid for a 21st century center of excellence program “Center for Diversity and Universality in Physics” and No. 18204015 by the Ministry of Education, Culture, Sports, Science and Technology of Japan. This research has made use of data obtained from the Data ARchive and Transmission System at ISAS/JAXA, the High Energy Astrophysics Science Archive Research Center at the NASA/Goddard Space



Flight Center, and the Two Micron All Sky Survey, which is a joint project of the University of Massachusetts and the Infrared Processing and Analysis Center/California Institute of Technology, funded by the National Aeronautics and Space Administration and the National Science Foundation. MSX was funded by the Ballistic Missile Defense Organization with additional support from NASA Office of Space Science. This research has also made use of the NASA/ IPAC Infrared Science Archive, which is operated by the Jet Propulsion Laboratory, California Institute of Technology, under contract with the National Aeronautics and Space Administration.

## References

- Albacete Colombo, J. F., Méndez, M., & Morrell, N. I. 2003, *MNRAS*, 346, 704
- Albacete Colombo, J. F., Flaccomio, E., Micela, G., Sciortino, S., & Damiani, F. 2007, *A&A*, 464, 211
- Anders, E., & Grevesse, N. 1989, *Geochim. Cosmochim. Acta*, 53, 197
- Bautz, M. W., Kissel, S. E., Prigozhin, G. Y., LaMarr, B., Burke, B. E., & Gregory, J. A. 2004, *Proc. SPIE*, 5501, 111
- Bearden, J. A. 1967, *Reviews of Modern Physics*, 39, 78
- Becklin, E. E., & Neugebauer, G. 1968, *ApJ*, 151, 145
- Benjamin, R. A., et al. 2003, *PASP*, 115, 953
- Berghoefer, T. W., Schmitt, J. H. M. M., Danner, R., & Cassinelli, J. P. 1997, *A&A*, 322, 167
- Broos, P. S., Feigelson, E. D., Townsley, L. K., Getman, K. V., Wang, J., Garmire, G. P., Jiang, Z., & Tsuboi, Y. 2007, *ApJS*, 169, 353
- Cappellari, M., & Copin, Y. 2003, *MNRAS*, 342, 345
- Catchpole, R. M., Whitelock, P. A., & Glass, I. S. 1990, *MNRAS*, 247, 479
- Cotera, A. S., Erickson, E. F., Colgan, S. W. J., Simpson, J. P., Allen, D. A., & Burton, M. G. 1996, *ApJ*, 461, 750
- Crowther, P. A., Hadfield, L. J., Clark, J. S., Negueruela, I., & Vacca, W. D. 2006, *MNRAS*, 372, 1407
- Cutri, R. M., et al. 2003, The IRSA 2MASS All-Sky Point Source Catalog, NASA/IPAC Infrared Science Archive. <http://irsa.ipac.caltech.edu/applications/Gator/>,
- Diehl, S., & Statler, T. S. 2006, *MNRAS*, 368, 497
- Egan, M. P., et al. 2003, *VizieR Online Data Catalog*, 5114, 0
- Ezuka, H., & Ishida, M. 1999, *ApJS*, 120, 277
- Feigelson, E. D., Broos, P., Gaffney, J. A., III, Garmire, G., Hillenbrand, L. A., Pravdo, S. H., Townsley, L., & Tsuboi, Y. 2002, *ApJ*, 574, 258
- Feigelson, E. D., et al. 2005, *ApJS*, 160, 379
- Figer, D. F., McLean, I. S., & Morris, M. 1999a, *ApJ*, 514, 202
- Figer, D. F., Kim, S. S., Morris, M., Serabyn, E., Rich, R. M., & McLean, I. S. 1999b, *ApJ*, 525, 750
- Figer, D. F., Rich, R. M., Kim, S. S., Morris, M., & Serabyn, E. 2004, *ApJ*, 601, 319
- Garmire, G. P., Bautz, M. W., Ford, P. G., Nousek, J. A., & Ricker, G. R., Jr. 2003, *Proc. SPIE*, 4851, 28

- Ghez, A. M., Salim, S., Hornstein, S. D., Tanner, A., Lu, J. R., Morris, M., Becklin, E. E., & Duchêne, G. 2005, *ApJ*, 620, 744
- Hamaguchi, K., et al. 2007, *ApJ*, 663, 522
- Hellier, C., & Mukai, K. 2004, *MNRAS*, 352, 1037
- Hyodo, Y., et al. 2008, *PASJ*, 60, #3182
- Imanishi, K., Koyama, K., & Tsuboi, Y. 2001, *ApJ*, 557, 747
- Imanishi, K., Nakajima, H., Tsujimoto, M., Koyama, K., & Tsuboi, Y. 2003, *PASJ*, 55, 653
- Inoue, H. 1985, *Space Science Reviews*, 40, 317
- Ishisaki, Y., et al. 2007, *PASJ*, 59, S113
- Jansen, F., et al. 2001, *A&A*, 365, L1
- Kim, S. S., Morris, M., & Lee, H. M. 1999, *ApJ*, 525, 228
- Kobayashi, Y., Okuda, H., Sato, S., Jugaku, J., & Dyck, H. M. 1983, *PASJ*, 35, 101
- Kokubun, M., et al. 2007, *PASJ*, 59, S53
- Koyama, K., Awaki, H., Kunieda, H., Takano, S., & Tawara, Y. 1989, *Nature*, 339, 603
- Koyama, K., Maeda, Y., Tsuru, T., Nagase, F., & Skinner, S. 1994, *PASJ*, 46, L93
- Koyama, K., Hamaguchi, K., Ueno, S., Kobayashi, N., & Feigelson, E. D. 1996a, *PASJ*, 48, L87
- Koyama, K., Maeda, Y., Sonobe, T., Takeshima, T., Tanaka, Y., & Yamauchi, S. 1996b, *PASJ*, 48, 249
- Koyama, K., et al. 2007a, *PASJ*, 59, S23
- Koyama, K., et al. 2007b, *PASJ*, 59, S221
- Koyama, K., et al. 2007c, *PASJ*, 59, S245
- Krabbe, A., et al. 1995, *ApJ*, 447, L95
- Krause, M. O., & Oliver, J. H. 1979, *Journal of Physical and Chemical Reference Data*, 8, 329
- Law, C., & Yusef-Zadeh, F. 2004, *ApJ*, 611, 858
- Maeder, A., & Meynet, G. 1987, *A&A*, 182, 243
- Mauerhan, J. C., Munro, M. P., & Morris, M. 2007, *ApJ*, 662, 574
- Mikles, V. J., Eikenberry, S. S., Munro, M. P., Bandyopadhyay, R. M., & Patel, S. 2006, *ApJ*, 651, 408
- Mitsuda, K., et al. 2007, *PASJ*, 59, S1
- Moneti, A., Stolovy, S., Blommaert, J. A. D. L., Figer, D. F., & Najarro, F. 2001, *A&A*, 366, 106
- Monnier, J. D., Tuthill, P. G., & Danchi, W. C. 1999, *ApJ*, 525, L97
- Morris, M., & Serabyn, E. 1996, *ARA&A*, 34, 645
- Morrison, R., & McCammon, D. 1983, *ApJ*, 270, 119
- Munro, M. P., et al. 2003, *ApJ*, 589, 225
- Munro, M. P., et al. 2004a, *ApJ*, 613, 326
- Munro, M. P., et al. 2004b, *ApJ*, 613, 1179
- Munro, M. P., Bower, G. C., Burgasser, A. J., Baganoff, F. K., Morris, M. R., & Brandt, W. N. 2006a, *ApJ*, 638, 183
- Munro, M. P., Bauer, F. E., Bandyopadhyay, R. M., & Wang, Q. D. 2006b, *ApJS*, 165, 173
- Murakami, H., Koyama, K., Sakano, M., Tsujimoto, M., & Maeda, Y. 2000, *ApJ*, 534, 283
- Murakami, H., Koyama, K., & Maeda, Y. 2001, *ApJ*, 558, 687

- Nagashima, C., et al. 1999, *Proceedings of Star Formation 1999*, ed. T. Nakamoto, Nobeyama Radio Observatory, 397
- Nagata, T., Woodward, C. E., Shure, M., Pipher, J. L., & Okuda, H. 1990, *ApJ*, 351, 83
- Nagata, T., Woodward, C. E., Shure, M., & Kobayashi, N. 1995, *AJ*, 109, 1676
- Nagayama, T., et al. 2003, *Proc. SPIE*, 4841, 459
- Nishiyama, S., et al. 2006, *ApJ*, 638, 839
- Okuda, H., et al. 1989, *The Center of the Galaxy*, 136, 281
- Okuda, H., et al. 1990, *ApJ*, 351, 89
- Oskinova, L. M., Ignace, R., Hamann, W.-R., Pollock, A. M. T., & Brown, J. C. 2003, *A&A*, 402, 755
- Ozawa, H., Grosso, N., & Montmerle, T. 2005, *A&A*, 438, 661
- Pollock, A. M. T., Corcoran, M. F., Stevens, I. R., & Williams, P. M. 2005, *ApJ*, 629, 482
- Portegies Zwart, S. F., Makino, J., McMillan, S. L. W., & Hut, P. 2001, *ApJ*, 546, L101
- Portegies Zwart, S. F., Makino, J., McMillan, S. L. W., & Hut, P. 2002a, *ApJ*, 565, 265
- Portegies Zwart, S. F., Pooley, D., & Lewin, W. H. G. 2002b, *ApJ*, 574, 762
- Predehl, P., & Schmitt, J. H. M. M. 1995, *A&A*, 293, 889
- Rana, V. R., Singh, K. P., Schlegel, E. M., & Barrett, P. E. 2006, *ApJ*, 642, 1042
- Schultheis, M., et al. 1999, *A&A*, 349, L69
- Serabyn, E., Shupe, D., & Figer, D. F. 1998, *Nature*, 394, 448
- Serlemitsos, P., et al. 2007, *PASJ*, 59, S9
- Skrutskie, M. F., et al. 2006, *AJ*, 131, 1163
- Smith, R. K., Brickhouse, N. S., Liedahl, D. A., & Raymond, J. C. 2001, *ApJ*, 556, L91
- Stevens, I. R., Blondin, J. M., & Pollock, A. M. T. 1992, *ApJ*, 386, 265
- Strüder, L., et al. 2001, *A&A*, 365, L18
- Takahashi, T., et al. 2007, *PASJ*, 59, S35
- Tawa, N., et al. 2008, *PASJ*, 60, #3170
- Terada, Y., Ishida, M., Makishima, K., Imanari, T., Fujimoto, R., Matsuzaki, K., & Kaneda, H. 2001, *MNRAS*, 328, 112
- Tsuboi, Y., Koyama, K., Sakano, M., & Petre, R. 1997, *PASJ*, 49, 85
- Tsuboi, Y., Koyama, K., Murakami, H., Hayashi, M., Skinner, S., & Ueno, S. 1998, *ApJ*, 503, 894
- Tsujimoto, M., et al. 2007a, *Proceedings of Suzaku Conference 2006*, *Progress of Theoretical Physics*, in press
- Tsujimoto, M., et al. 2007b, *ApJ*, 665, 719
- Turner, M. J. L., et al. 2001, *A&A*, 365, L27
- Tuthill, P. G., Monnier, J. D., & Danchi, W. C. 1999, *Nature*, 398, 487
- Tuthill, P., Monnier, J., Tanner, A., Figer, D., Ghez, A., & Danchi, W. 2006, *Science*, 313, 935
- van der Hucht, K. A., Cassinelli, J. P., & Williams, P. M. 1986, *A&A*, 168, 111
- Wang, Q. D., Gotthelf, E. V., & Lang, C. C. 2002, *Nature*, 415, 148
- Wang, Q. D., Dong, H., & Lang, C. 2006, *MNRAS*, 371, 38
- Weisskopf, M. C., Brinkman, B., Canizares, C., Garmire, G., Murray, S., & Van Speybroeck, L. P. 2002, *PASP*, 114, 1
- Werner, M. W., et al. 2004, *ApJS*, 154, 1

- Williams, P. M., van der Hucht, K. A., & The, P. S. 1987, A&A, 182, 91
- Yamauchi, S., Kawada, M., Koyama, K., Kunieda, H., & Tawara, Y. 1990, ApJ, 365, 532
- Yusef-Zadeh, F., Law, C., Wardle, M., Wang, Q. D., Fruscione, A., Lang, C. C., & Cotera, A. 2002, ApJ, 570, 665